Research Square

Preprints are preliminary reports that have not undergone peer review.
They should not be considered conclusive, used to inform clinical practice,
or referenced by the media as validated information.

The diagnostic performance of dual phase [^{99m}Tc]-MIBI SPECT/CT in primary hyperparathyroidism assessment: limits and prediction model of false negative result considering pre-scan data in a single center experience

Pietro Bellini
pietro.bellini@asst-spedalicivili.it
ASST Spedali Civili Brescia
Giada Bianchetti
ASST Spedali Civili
Francesco Dondi
University of Brescia, ASST Spedali Civili Brescia
Chiara Ingraito
ASST Spedali Civili
Carlo Alberto Rodella
ASST Spedali Civili
Francesca Saiani
ASST Spedali Civili
Davide Lancini
University of Brescia
Elisa Gatta
University of Brescia, ASST Spedali Civili di Brescia
Riccardo Morandi
University of Brescia, ASST Spedali Civili
Davide Lombardi
University of Brescia
Silvia Lucchini
ASST Spedali Civili Brescia
Carlo Cappelli
University of Brescia, ASST Spedali Civili di Brescia
Luigi Spiazzi
ASST Spedali Civili
Cesare Piazza
University of Brescia
Claudio Casella
University of Brescia, ASST Spedali Civili
Francesco Bertagna
University of Brescia, ASST Spedali Civili Brescia

Research Article

Keywords: primary hyperparathyroidism (PHPT), [99mTc]Tc-MIBI Scintigraphy, SPECT/CT imaging, logistic regression, predictive model, diagnostic predictors

Posted Date: September 20th, 2026

DOI: https://doi.org/10.21203/rs.3.rs-10646180/v1

License: This work is licensed under a Creative Commons Attribution 4.0 International License. Read Full License

Additional Declarations: No competing interests reported.

Abstract

Purpose

Primary hyperparathyroidism (PHPT) is a prevalent endocrine disorder characterized by abnormal secretion of parathyroid hormone (PTH), primarily arising from single parathyroid adenomas or hyperplasia. The primary

treatment involves surgical excision, necessitating accurate pre-operative localization.

Methods

This research evaluates the outcomes of dual-phase [^{99m}Tc]Tc-MIBI scintigraphy SPECT/CT in PHPT and its association with pre-scan radiological and biochemical parameters. Indeed, despite its common use, [^{99m}Tc]Tc-MIBI scintigraphy exhibits limitations, leading to false-negative results in approximately 25% of cases. Our monocentric study focuses on identifying predictors of false-negative results, considering clinical, biochemical, and morphological parameters, through the application of a logistic regression model.

Results

The study reveal a significant associations between neck ultrasound results, calcemia, and true positive scintigraphy outcomes. A probability assessment for false-negative results is proposed, offering clinicians a valuable tool for decision support with a model identifying the 71.8 of potential false negative cases.

Conclusion

While acknowledging the need for further refinement and expanded cohorts, our findings contribute valuable insights to the diagnostic landscape of PHPT, offering a personalized approach to guide clinicians in optimal diagnostic pathways.

1. Introduction

Primary hyperparathyroidism (PHPT) is a prevalent endocrine disorder characterized by hyperfunctioning parathyroid glands that exhibit abnormal secretion of parathyroid hormone (PTH) [1, 2]. In the majority of cases, the condition arises from a single parathyroid adenoma or hyperplasia (85–87%), although involvement of multiple glands (12–15%), or exceptionally, parathyroid carcinoma (< 1%) is also plausible [3, 4].

Approximately 95% of PHPT cases are sporadic, with only 5% attributed to hereditary factors, typically associated with multiple endocrine neoplasia (MEN) types 1, 2, and 4 [3]. Patients are often asymptomatic, and diagnosis commonly occurs incidentally during routine blood tests or neck ultrasounds conducted for other purposes. PHPT is frequently linked to hypercalcemia (HC), hypophosphatemia (hF), hypercalciuria, and an increase in the size of the affected parathyroid gland. If left untreated, PHPT may lead to complications related to calcium metabolism, such as nephrocalcinosis and osteoporosis [5].

Although surgically excising of the hyperfunctioning gland is an option for all patients, it is recommended when serum calcium exceeds the upper normal limit by more than 1 mg/dL, if skeletal or renal involvement is present, or in patients under the age of 50 [6].

In this cases, pre-operative imaging examinations are routinely conducted [5]. Precise localization of the involved parathyroid is crucial for enabling minimally invasive surgery [7]. Currently, neck ultrasound (NUS) and dual-phase ^{99m}Tc-hexakis-2-methoxyisobutyl isonitrile ([^{99m}Tc]Tc-MIBI) scintigraphy, coupled with single photon emission computed tomography/computed tomography (SPECT/CT), are the most commonly used and recommended pre-operative imaging techniques [8]. These methods exhibit respective sensitivities (SE) of 76.1% and 78.9%, and positive predictive values (PPV) of 93.2% and 90.7% [9].

Notably, conventional imaging may yield false negative results in approximately one in four patients. In such instances, secondary examinations, including dedicated 4D-CT and [^{18}F]-fluorocholine positron emission tomography/computed tomography (PET/CT), may be warranted. Despite higher costs and limited availability, these alternatives demonstrate higher SE, approximately 89.4% [10] and 90–93% [10–12], respectively.

In this perspective, this research seeks to evaluate the association between the outcomes of dual-phase [^{99m}Tc]Tc-MIBI scintigraphy SPECT/CT and the pertinent pre-scan radiological and/or biochemical information, with the primary aim to establish criteria for discerning a specific patient subset, thus facilitating the initiation of more sensitive secondary examinations early in the diagnostic process.

2. Materials and Methods

2.1 Selection of patients

This investigation involved a retrospective analysis of 177 patients who underwent dual-phase [^{99m}Tc]Tc-MIBI scintigraphy and subsequent SPECT/CT between May 2018 and June 2019. Informed consent was obtained from all participants included in the study, with the exclusion of patients who had died or could not be contacted, in accordance with the Ethical Committee's approval due to the retrospective nature of the study. The study adhered to the Declaration of Helsinki guidelines and received approval from the local Ethics Committee (protocol number 0065600/25). All patients performed a neck ultrasound before the scan. Exclusions were made for patients with chronic kidney disease (CKD), specifically those with a glomerular filtration rate (GFR) below 45 mL/min/1.73m², as well as individuals with a history of kidney transplant in order to exclude patients with suspect of secondary hyperparathyroidism. In addition, only patients with a confirmed histological or radiological diagnosis of a single parathyroid adenoma or hyperplasia were included.

Histological diagnoses were always made after surgery, while radiological diagnoses were made after dedicated 4D-CT, the available examination with the highest SE and PPV. No [^{18}F]-fluorocholine PET/CT was performed because, despite literature reports and international guidelines, the Italian National Health System did not yet guarantee this examination before 2021. Finally, the study included 64 Patients.

2.2 SestaMIBI SPECT/CT Imaging and Interpretation

Each patient received an intravenous injection of 740 Mbq (± 10%) of [^{99m}Tc]Tc-MIBI, following international guidelines [13]. All participants underwent the examination after discontinuing therapy with potential interference [13].

Planar images of the neck and thorax in anterior projection were captured at 10 and 90 minutes (± 5 minutes) post-injection. Subsequently, a SPECT/CT of the same anatomical region was conducted. The imaging procedures were carried out using a Discovery 670 NM/CT tomograph (General Electric Company, GE, Milwaukee, Wisconsin) with standard parameters. For static images, a low-energy high-resolution (LEHR) parallel hole collimator, 128x128 matrix, zoom 1.5x, acquisition time 600s, and energy window 140 keV ± 10% were employed. SPECT/CT images were acquired using LEHR parallel hole collimators, 128x128 matrix, zoom 1.5x, 3° step with 15s/step, energy window 140 keV ± 10%, scatter 120 keV ± 10% and Tc parameters 20 Kv, 80 mA, slice thickness 2.5 mm, with reconstruction performed using standard settings, a matrix of 512, and DFOV 50.

The qualitative assessment of both planar and tomographic images was conducted by two expert physicians (FD; PB).

2.3 Data Collection

We examined the results of [^{99m}Tc]Tc-MIBI scintigraphy and SPECT/CT, alongside the compilation of clinical (osteoporosis presence, vitamin D treatment), biochemical (PTH, calcemia, phosphatemia, and 25(OH)-vitamin D levels), and morphological (ultrasound-measured parathyroid diameter) data. Due to constraints in data collection for every patient, it is noteworthy that osteoporosis presence was assessed in 38 patients, vitamin D treatment in 46 patients, phosphatemia in 38 patients, and 25(OH)-vitamin D levels in 40 patients. Moreover, among the 64 patients who underwent NUS before scintigraphy, parathyroid diameter was measured in 40 cases.

2.4 Data Elaboration and Statistical Analysis

Statistical analyses were conducted using Python programming language (https://www.python.org/). Categorical variables were presented as simple and relative frequencies, while numeric variables were summarized using mean, minimum, and maximum values.

Differences between variables were assessed utilizing the two-tailed chi-squared test (χ^2) for categorical variables and Student's t-test for numeric variables. The correlation between variables was evaluated using the Pearson correlation coefficient (PCC). The PCC assesses the linear relationship between two continuous variables, providing a measure of the strength and direction of the correlation. A significance threshold of $p < 0.05$ was considered to indicate statistical significance.

To ascertain the potential of clinical and biochemical factors as indicators of potential false negatives in [^{99m}Tc]Tc-MIBI results, logistic regression analysis was employed.

Logistic regression analysis was performed using Python, leveraging the statsmodels (https://pypi.org/project/statsmodels/) and scikit-learn (https://pypi.org/project/scikit-learn/) libraries. The statsmodels library was employed for statistical analysis, providing detailed information about the regression model, including coefficients and p-values. Additionally, the scikit-learn library facilitated model training and evaluation, offering tools for predictive modeling and machine learning.

The binary outcome in our study was defined by the presence or absence of false negatives in the [^{99m}Tc]Tc-MIBI results (assigned as 0 if a false negative occurred and 1 if a true positive occurred). Through the calculation of coefficients, logistic regression provides insights into the association between predictor variables and the likelihood of false negatives. Subsequently, the predictive ability of the trained model was evaluated by constructing receiver operating characteristic (ROC) curves and confusion matrix.

Finally, the probability of obtaining a false-negative result was calculated for each patient.

3. Results

3.1. Characteristics of population

The study included 64 patients (55 females and 9 males, with an average age of 67.1 ± 11.2 years) with final diagnosis of parathyroid adenoma or hyperplasia. Among them, 48 received a histological, and 16 were diagnosed radiologically by 4D-CT. Further details regarding patient characteristics are outlined in the following Table 1.

Table 1
Characteristics of the population and data collection

Age (years)	**Mean ± SD (range)**	**n/N (%)**	**/**
	67.1 ± 11.2 (13–83)	**/**	**/**
Gender			
Females	/	55/64 (85.9%)	/
Males	/	9/64 (14.1%)	
[^{99m}Tc]Tc-MIBI scintigraphy result			/
Positive	/	40/64 (62.5%)	
Negative	/	24/64 (37.5%)	
Diagnosis confirmation			
Histological	/	48/64 (75%)	/
Radiological	/	16/64 (25%)	
Neck ultrasound result			
Positive	/	40/64 (62.5%)	/
Negative	/	24/64 (37.5%)	
	Positive Scintigraphy	**Negative Scintigraphy**	**p value**
PTH (pg/mL)	178.77 ± 118.06 (72–646)	119.35 ± 44.36 (58.1–216)	**0.021**
Calcemia (mg/dL)	10.91 ± 0.86 (9.3–13.9)	10.35 ± 0.60 (9.47–11.63)	**0.007**
Creatinine	0.88 ± 0.28(0.56–1.53)	0.85 ± 0.23(0.48–1.41)	> 0.05
Parathyroid major diameter (mm)*	13.92 ± 7.82 (4.5–41.0)	8.50 ± 3.20 (5.0–15.0)	**0.036**
Phosphatemia (mg/dL)**	2.50 ± 0.45 (1.7–3.3)	2.51 ± 0.44 (1.7–3.3)	> 0.05
25(OH)VitD (ng/mL)***	26.66 ± 14.44 (7.0–83.0)	27.09 ± 14.52 (7.7–83.0)	> 0.05
Osteoporosis******	19/25 (76%)	9/13 (69.23%)	> 0.05
VitD therapy*******	22/29 (75.86%)	12/17 (70.59%)	> 0.05

* 40 patients with positive ultrasound

** 38 patients

*** 40 patients

**** 38 patients

***** 46 patients

SD = standard deviation ; n = number; N = total number of patients

Among the 64 patients, 40 presented a suspect of enlarged parathyroid during pre-examination NUS, while 24 had a negative NUS (Table 1). In addition, 40 of them (64%) had a true positive [^{99m}Tc]Tc-MIBI scintigraphy and SPECT/CT, while the remaining 24 (36%) had a false negative results (Table 1). Ten out of twenty patients (50%) with a negative NUS had a positive scintigraphy, while ten out of twenty patients (50%) with a negative scintigraphy had a previous positive NUS. No discordant results were found when NUS and scintigraphy were both positive. Just one ectopic adenoma was found.

A higher, although not significant (p-value = 0.062), probability of positive results (y-axis = 1) at [^{99m}Tc]Tc-MIBI examination in patients with positive ultrasound (29 of the 40 patients, corresponding to 72.50%), while 13 of the 24 patients with negative ultrasound (x-axis = 0, 54.17%) showed a false negative [^{99m}Tc]Tc-MIBI result (y-axis = 0), as represented in Fig. 1.

Concerning biochemical data, the statistical analysis revealed a significant difference in mean calcemia levels between patients with true positive [^{99m}Tc]Tc-MIBI scintigraphy and SPECT/CT results (10.91 ± 0.86 mg/dL) and those with false negative scans (10.35 ± 0.60 mg/dL) (p-value = 0.007). Similarly, the distribution of parathyroid hormone (PTH) levels indicating significantly higher mean values in patients with positive [^{99m}Tc]Tc-MIBI results (178.77 ± 118.06 pg/mL) compared to those with negative results (119.35 ± 44.36 pg/mL) (p-value = 0.021).

Concerning the 40 patients with positive ultrasound, a significantly higher major diameter of the enlarged parathyroid detected by the radiological examination was found in patients with positive [^{99m}Tc]Tc-MIBI scintigraphy (13.92 ± 7.82 vs 8.50 ± 3.20 mm ; p value = 0.036). Despite this quite strong correlation, no further analysis in the sub-group was performed due to the limitation of the sample. Considering the same limitation, no other significant relation between pre-scan data collected and [^{99m}Tc]Tc-MIBI scintigraphy result was found.

3.2. Assessment of the dependence between variables

Considering the statistical association between true positive [^{99m}Tc]Tc-MIBI scintigraphy and SPECT/CT results and elevated mean calcemia and PTH values compared to those with false negative scans, we delved further into the relationship between these variables.

The investigation revealed a statistically significant and moderately strong positive linear correlation between calcemia and PTH with a Pearson correlation coefficient of 0.675 (p-value = $9.6e^{-10}$). This correlation underscores the association between calcemia and PTH levels, underlying their interplay in the context of [^{99m}Tc]Tc-MIBI scintigraphy outcomes. This relation is visually represented in the scatter plot in Fig. 2.

Moreover, our analysis was expanded to explore the relationship between ultrasound outcomes and the levels of calcemia and PTH, as illustrated in Fig. 3.

In Fig. 3a, the distribution of calcemia is depicted for patients with negative (0) and positive (1) neck ultrasound results. Surprisingly, this examination revealed that the ultrasound outcome did not demonstrate a statistically significant correlation with calcium levels (p value = 0.811). Similarly, Fig. 3b presents a box plot showcasing the values of parathyroid hormone in relation to the neck ultrasound findings, with the same result (p value = 0.620).

3.3. Evaluation of the predictive potential of morphological and biochemical variables in [^{99m}Tc]Tc-MIBI scintigraphy outcomes

In light of the compelling insights derived from our analysis, we aimed to ascertain the potential of predicting false-negative outcomes through the utilization of available morphological or biochemical data. Within this framework, our primary objective was to pinpoint variables that could significantly predict the [^{99m}Tc]Tc-MIBI scintigraphy result. Subsequently, we investigated the feasibility and precision of assessing the risk of false positives by logistic regression: this method is useful for predicting the likelihood of a patient having a specific medical condition based on diverse factors, even with limited datasets.

In order to investigate the relationship between calcemia, PTH and NUS outcome and the likelihood of false-negative results in [^{99m}Tc]Tc-MIBI scintigraphy, we analysed the different possible combinations of these factors. The coefficients obtained from the logistic regression models, together with the 98% confidence interval, were schematized in the following Table 2.

Table 2
Comparison of coefficients, confidence intervals (CI), and p-values obtained for the different evaluated models.

Variable	MODEL 1			MODEL 2			MODEL 3			MODEL 4		
	coeff	CI [0.025–0.975]	p-value	coeff	CI [0.025–0.975]	p-value	coeff	CI [0.025–0.975]	p-value	coeff	CI [0.025–0.975]	p-value
intercept	0.0193	[-0.887-0.926]	0.967	-0.2261	[-1.130-0.678]	0.624	0.7882	[0.132–1.445]	0.019	-0.0418	[-1.016-0.932]	0.933
PTH (pg/mL)	1.2268	[0.069–2.385]	**0.038**				0.9017	[-0.299-2.103]	0.141	0.8237	[-0.431-2.078]	0.198
Calcemia (mg/dL)				1.0523	[0.278–1.827]	**0.008**	0.7048	[-0.095-1.505]	0.084	0.8237	[-0.031-1.689]	0.059
Ultrasound result	1.1803	[0.050–2.310]	0.041	1.4126	[0.212–2.613]	0.021				1.3469	[0.135–2.559]	**0.029**
Accuracy	0.688 ± 0.065			0.718 ± 0.081			0.549 ± 0.082			0.702 ± 0.091		

Table 2 compares the coefficients, the 98% confidence interval, and the p-values for four different logistic regression models, each exploring different combinations of input parameters.

As can be seen looking at the Table 2, Model 1 includes PTH and NUS results, Model 2 involves calcemia and NUS result, Model 3 incorporates PTH and calcemia, and model 4 combines all the three variables.

In Model 1, both PTH and ultrasound results demonstrate a significant positive association with the true positive MIBI outcome, featuring coefficients of 1.2268 for PTH (p-value = 0.038) and 1.1803 for the NUS result (p-value = 0.041). Similarly, Model 2 highlights a substantial positive association of calcemia (coeff = 1.0523, p-value = 0.008) and NUS result (coeff = 1.4126, p-value = 0.021) with the positive outcome of the scintigraphy.

Interestingly, when considering PTH and calcemia together in Model 3 and Model 4, these variables do not exhibit a significant correlation with the outcome.

To evaluate model performance, we applied the k-fold cross-validation technique, with k = 5: the dataset is thus partitioned into k equally sized folds, and the model is trained k times, each time using k-1 folds for training and the remaining fold for testing. The last row shows the mean accuracy ± SD of each model, calculated by averaging the cross-validation scores.

Examining the accuracies, the first model, incorporating PTH and ultrasound results, achieves an accuracy of 0.688 ± 0.065. In the second model, where calcemia and ultrasound results are considered, the accuracy increases slightly to 0.718 ± 0.081. However, the third model, which includes both PTH and calcemia, exhibits a noticeably lower accuracy of 0.549 ± 0.082 and the fourth model, encompassing all three variables, shows an improved accuracy of 0.702 ± 0.091.

3.4. Evaluation of potential clinical relevance of Model 2 through additional metrics and the definition of a patient-associated false-negative risk

We selected Model 2 as the best predictor of scintigraphy result for further evaluation.

The confusion matrix is represented in Fig. 4a and ROC curve analysis in Fig. 4b.

The confusion matrix for the evaluated model reveals a total of 35 true positive instances, 12 true negative cases and also 5 false negative and 12 false positive predictions. The ROC curve for the Model 2 demonstrates promising characteristics, with an AUC value of 0.768. Moreover the practical implications of the obtained coefficients were analyzed employing them to calculate the probability associated with each patient's likelihood of experiencing a false-negative [^{99m}Tc]Tc-MIBI result based on their morphological and biochemical parameters.

The probability of obtaining a false-negative result $P\,(Y=0)$ is calculated as the inverse of the logistic function (sigmoid) applied to the linear combination of the model's coefficients and the corresponding values of morphological and biochemical parameters for each patient, according to the formula:

$$P\ (Y=0) = 1 - \frac{1}{1+e^{-(\beta_0+\beta_1 x_1+\beta_2 x_2)}}$$

where Y is the [^{99m}Tc]Tc-MIBI result, β_0 is the intercept, and β_1, β_2 are the coefficients associated with the predictor variables x_1, x_2, corresponding in our model to calcemia levels and ultrasound result, respectively

The probability values, together with the [^{99m}Tc]Tc-MIBI result (0 = false-negative, 1 = true-positive), calculated for each patient, are reported in the following Table 3.

Table 3

The probability of negative result calculated for each patient with the trained logistic model (Model 2) is reported in table (P(Y = 0)). The third column shows the effective result of scintigraphy, while the last column reveals the accordance of model's prediction with the real result: a threshold of 50% probability was applied: if the calculated probability of obtaining a false negative was below 50%, the model assigned a class 1 (true positive), while probabilities above 50% were assigned class 0 (false negative [^{99m}Tc]Tc-MIBI result)

Patient ID	P(Y = 0) [%]	[^{99m}Tc]Tc-MIBI result	Accordance with model	Patient ID	P(Y = 0) [%]	[^{99m}Tc]Tc-MIBI result	Accordance with model
001	81.9	1	FALSE	033	29.5	1	TRUE
002	79.1	0	TRUE	034	28.8	1	TRUE
003	54.7	1	FALSE	035	27.0	1	TRUE
004	54.4	0	TRUE	036	26.6	0	FALSE
005	76.6	0	TRUE	037	49.9	1	TRUE
006	53.1	0	TRUE	038	47.8	0	FALSE
007	74.6	0	TRUE	039	47.2	1	TRUE
008	49.0	0	FALSE	040	24.6	1	TRUE
009	46.8	0	FALSE	041	24.6	1	TRUE
010	46.3	1	TRUE	042	22.6	0	FALSE
011	70.1	0	TRUE	043	22.6	1	TRUE
012	68.0	1	FALSE	044	22.6	1	TRUE
013	41.8	1	TRUE	045	43.0	0	TRUE
014	66.1	0	TRUE	046	43.0	1	TRUE
015	41.0	0	FALSE	047	21.4	1	FALSE
016	38.4	0	FALSE	048	20.8	0	TRUE
017	36.9	1	TRUE	049	20.8	1	FALSE
018	36.4	1	TRUE	050	38.8	0	FALSE
019	35.9	1	TRUE	051	34.3	1	TRUE
020	60.3	0	TRUE	052	15.9	1	TRUE
021	34.6	1	TRUE	053	14.9	0	FALSE
022	59.3	0	TRUE	054	14.5	1	TRUE
023	33.4	0	FALSE	055	13.2	1	TRUE
024	32.7	1	TRUE	056	27.6	1	TRUE
025	56.7	0	TRUE	057	27.4	1	TRUE
026	32.2	1	TRUE	058	27.4	1	TRUE
027	56.4	0	TRUE	059	26.7	0	FALSE
028	31.5	1	TRUE	060	9.9	1	TRUE
029	31.1	1	TRUE	061	21.4	1	TRUE
030	31.1	1	TRUE	062	6.1	1	TRUE
031	31.1	1	TRUE	063	8.1	1	TRUE
032	30.4	1	TRUE	064	1.1	1	TRUE

In Table 3, each row corresponds to a unique patient identifier (Patient ID) from 001 to 064.

Looking at the probability values obtained, we can observe that in 14 patients the probability to obtain a false-negative result is higher than the 50% threshold, and, among them, only 3 (21.4%) were misclassified. Similarly, among the 50 patients with a lower risk to obtain a false-negative result (P(Y = 0) < 50%), 37, corresponding to 74%, were correctly identified by the model.

4. Discussion

The detection and localization of parathyroid disease in PHPT with surgical indication pose a significant challenge, particularly given the limitations of the first line imaging examination represented by NUS and [^{99m}Tc]Tc-MIBI dual-phase scintigraphy and SPECT/CT. Despite the availability of examinations with higher spatial resolution such as 4D-CT, which in our study was used as a gold standard for the diagnosis of parathyroid adenoma/hyperplasia in absence of histological examination [14], and [^{18}F]-fluorocholine PET/CT, current recommendations in Italy endorse the use of PET only after negative or doubtful results from [^{99m}Tc]Tc-MIBI scintigraphy. Furthermore, the literature indicates that specific parameters, including PTH levels, calcemia, and parathyroid diameters, have the potential to significantly impact the outcomes of [^{99m}Tc]Tc-MIBI scintigraphy. Consequently, it is possible to hypothesise a prediction of the scintigraphy result based on these parameters [15, 16]. Given the cost implications in terms of finances, absorbed dose by patient and time associated with conducting this examination and another subsequent imaging in cases of negative results, it would be beneficial to establish a robust method that would enable a seamless transition to a more sensitive and in-depth investigation, should this be justified by a high risk of negative or doubtful results.

The aim is to enhance diagnostic accuracy and optimize resource limiting the utilization of [^{99m}Tc]Tc-MIBI scintigraphy when it could be really useful. In this perspective, we conducted a thorough evaluation within the framework of this monocentric study to investigate clinical, biochemical, and morphological parameters that could serve as significant predictors of the scintigraphy result, particularly false negative result. In line with existing literature and substantiated by our own data (see Section 3.1 and 3.2), we focused on variables available for the majority of included patients, consistently demonstrating a substantial correlation with the outcomes of [^{99m}Tc]Tc-MIBI scintigraphy, namely the pre-examination neck ultrasound result, PTH, and calcemia. Although the ultrasound diameter of the adenoma or parathyroid hyperplasia shows a discernible correlation with MIBI outcome, attributable to the well-recognized spatial resolution constraints of scintigraphy and SPECT, it has not been taken into account due to insufficient sample size (only 40 patients of 64). This correlation suggests that in instances of diminished dimensions, a false-negative result might be hypothesized due to the imaging system's limited resolving capabilities.

To assess the significance of the selected parameters, we employed a logistic regression model, widely used in medical research, particularly in scenarios where the outcome of interest is binary, due to its ability to model the probability of an event occurring [17]. Table 2 provides a comprehensive comparison of the logistic regression models, shedding light on the interplay between the selected variables and the outcomes of [^{99m}Tc]Tc-MIBI scintigraphy. Model selection was a nuanced process guided by both statistical significance and practical interpretability. Model 1, featuring PTH and ultrasound results, showcases a significant positive association with the true positive MIBI outcome. Similarly, Model 2, involving calcemia and ultrasound results, reveals a positive correlation with the scintigraphy's positive outcome. Intriguingly, when PTH and calcemia are combined in Models 3 and 4, their lack of significant correlation with the outcome is notable. This absence of significance is likely linked to the positive correlation observed between PTH and calcemia, suggesting potential multicollinearity challenges.

The decision to favor Model 2 was underpinned by its superior accuracy, as evidenced by the k-fold cross-validation results. Model 2, considering calcemia and ultrasound results, exhibited an accuracy of 0.718 ± 0.081, outperforming other models. In Model 2, both the ultrasound neck result and calcemia exhibit statistical significance, with a p-value of 0.021 for ultrasound and 0.008 for calcemia, respectively. Neck ultrasound can be considered as a representation of lesion dimensions and position, with the hypothesis that a negative ultrasound result may harbor smaller parathyroid gland diseases or a parathyroid localized in an ectopic or deep site [18].

Regarding calcemia, its regulation involves multiple mechanisms, and parathyroid hyperfunction is one of the most significant causes of elevated serum calcium levels. Moreover, "out of range" calcemia could one of the initial signs of PHPT, even though it may remain within the physiological range in the early phase of the disease [18]. Studies diverge in defining the role of calcemia in predicting the outcomes of [^{99m}Tc]Tc-MIBI dual-phase scintigraphy and SPECT/CT; while some find a significant relationship [18, 19], others do not confirm it [20]. In our study, calcium levels exhibited a significant predictive capability of [^{99m}Tc]Tc-MIBI scintigraphy result, with higher levels associated with a higher probability of a true positive outcome (p-value = 0.007). Furthermore, in patients with calcium levels within the physiological range or just slightly above the upper physiological limit, the traditional nuclear medicine examination yielded false-negative results in over 50% of patients with true PHPT.

PTH is the principal hormone produced by parathyroid glands, reflecting their activity, and our study revealed a significant (p-value = 0.021) correlation between PTH levels and the outcomes of [^{99m}Tc]Tc-MIBI dual-phase scintigraphy and SPECT/CT (Table 1). The data in question is well documented and likely indicative of a nonspecific mechanism of cellular MIBI uptake, potentially associated with mitochondrial activity and subsequent cellular function. This phenomenon may be linked to the increased production of PTH in cells within the adenoma or hyperplastic parathyroid [21].

However, since our analysis indicated a strong (PPC = 0.675) and significant (p-value < 0.0001) correlation between PTH and calcemia, the inclusion of both variables in the logistic regression model did not provide additional value, diminishing the predictive capacity of the model as could be showed by Model 3 and 4.

Overall, the proposed logistic regression model, selected based on its superior accuracy in predicting [^{99m}Tc]Tc-MIBI scintigraphy outcomes, demonstrated a commendable predictive capacity, classifying cases correctly in 71.8% of the proposed instances. These promising results suggest the model's potential utility as a predictive tool. However, it is important to note that the limited number of available data points may have influenced the model's performance. The two main limitations of our study are the small patient sample size and the limited number of parameters considered. One avenue for improvement would be to include a larger number of patients, potentially by extending the study's inclusion period and/or including other centres. Taking into account the major axis of the adenoma as detected by ultrasound could contribute to a more robust and generalisable model.

Furthermore, the model provides a probability value for the likelihood of obtaining a false-negative result for each patient. This aspect is particularly valuable as it offers clinicians an additional tool for decision support. By assessing the probability revealed by the model, healthcare professionals can gauge the feasibility of moving directly to a more specific investigation. This individualized probability assessment enhances the clinical utility of the logistic regression model, aiding physicians in making informed decisions about the necessity of further, potentially more sensitive, diagnostic procedures and optimize the diagnostic algorithms in the management of the PHPT with a potentially surgical indication.

5. Conclusions

[^{99m}Tc]Tc-MIBI scintigraphy in the detection and localization of parathyroid diseases in PHPT present known limitations and our findings underscore the influence of certain parameters on its outcomes. Although the proposed logistic regression model has demonstrated promising predictive accuracy, further refinement and enhanced generalisability appear necessary, particularly as the patient cohort and parameters considered expand. In addition, a prospective study with a larger sample size could introduce a valuable dimension to clinicians' decision-making processes by providing a probability assessment for false-negative results. This could potentially allow for earlier imaging examinations with higher SE in selected subgroups of patients.

Declarations

Compliance with Ethical Standards

Ethical approval: The study adhered to the Declaration of Helsinki guidelines and received approval from the local Ethics Committee (protocol number 0065600/25)

Funding:

This research received no external funding.

Acknowledgments: nothing to declare.

Conflicts of Interest: The authors declare no conflicts of interest.

Author Contribution

conceptualization, P.B., G.B. and S.L.;methodology, P.B. and G.B.;software, G.B.; validation, P.B., G.B., F.D. and F.B.; formal analysis, G.B. and P.B.; investigation, P.B.; resources, n.d.; data curation, P.B., G.B.; writing—original draft preparation, P.B., G.B., E.G., R.M.; writing—review and

editing, F.B., D.L., C.P., Cl.Ca., Ca.Ca, C.I., D.L., L.S., C.a.R., F.S.; visualization, P.B., R.M., E.G.; supervision, F.B., D.L., C.P., Cl.Ca., Ca.Ca, L.M., L.S.; project administration, P.B.;

References

1. M. Muñoz-Torres, A. García-Martín, Primary Hyperparathyroidism. Med. Clin. (Barc). **150**, 226–232 (2018). 10.1016/j.medcli.2017.07.020
2. G.J. Kowalski, G. Bu?a, D. ??d?o, A. Gawrychowska, Gawrychowski, J. Prim. Hyperparathyroidism Endokrynologia Polska. **71**, 260–270 (2020). 10.5603/EP.a2020.0028
3. F. Carral, A.I. Jiménez, M. Tomé, J. Álvarez, A. Díez, F. Partida, C. Ayala, Factors Associated with Negative 99mTc-MIBI Scanning in Patients with Primary Hyperparathyroidism. Revista Española de Med. Nuclear e Imagen Mol. (English Edition). **40**, 222–228 (2021). 10.1016/j.remnie.2021.01.007
4. A. Galani, R. Morandi, M. Dimko, S. Molfino, C. Baronchelli, S. Lai, F. Gheza, C. Cappelli, C. Casella, Atypical Parathyroid Adenoma: Clinical and Anatomical Pathologic Features. World J. Surg. Onc. **19**, 19 (2021). 10.1186/s12957-021-02123-7
5. G.G. Callender, R. Udelsman, Surgery for Primary Hyperparathyroidism. Cancer. **120**, 3602–3616 (2014). 10.1002/cncr.28891
6. J.P. Bilezikian, A.A. Khan, S.J. Silverberg, G.E. Fuleihan, C. Marcocci, S. Minisola, N. Perrier, A. Sitges-Serra, R.V. Thakker, G. Guyatt, M. Mannstadt, J.T. Potts, B.L. Clarke, M.L. Brandi, International Workshop on Primary Hyperparathyroidism,. Evaluation and Management of Primary Hyperparathyroidism: Summary Statement and Guidelines from the Fifth International Workshop. J Bone Miner Res. 2022;37(11):2293–2314. 10.1002/jbmr.4677. Epub 2022 Oct 17. PMID: 36245251
7. E. Battistella, L. Pomba, R. Toniato, M. Burei, M. Gregianin, S. Watutantrige Fernando, A. Toniato, Evolution of the Diagnosis and Treatment of Primary Hyperparathyroidism. JCM 2023, 12, 2057. 10.3390/jcm12052057
8. G. Treglia, R. Sadeghi, C. Schalin–Jäntti, C. Caldarella, L. Ceriani, L. Giovanella, D.W. Eisele, Detection Rate of 99m Tc-MIBI Single Photon Emission Computed Tomography (SPECT)/CT in Preoperative Planning for Patients with Primary Hyperparathyroidism: A Meta-analysis. Head Neck. **38** (2016). 10.1002/hed.24027
9. K. Cheung, T.S. Wang, F. Farrokhyar, S.A. Roman, J.A. Sosa, A Meta-Analysis of Preoperative Localization Techniques for Patients with Primary Hyperparathyroidism. Ann. Surg. Oncol. **19**, 577–583 (2012). 10.1245/s10434-011-1870-5
10. A. Cuderman, K. Senica, S. Rep, M. Hocevar, T. Kocjan, M.J. Sever, K. Zaletel, L. Lezaic, 18 F-Fluorocholine PET/CT in Primary Hyperparathyroidism: Superior Diagnostic Performance to Conventional Scintigraphic Imaging for Localization of Hyperfunctioning Parathyroid Glands. J. Nucl. Med. **61**, 577–583 (2020). 10.2967/jnumed.119.229914
11. V. Pretet, M. Rotania, M. Helali, M. Ignat, M. Vix, A. Imperiale, 18F-Fluorocholine PET and Multiphase CT Integrated in Dual Modality PET/4D-CT for Preoperative Evaluation of Primary Hyperparathyroidism. JCM 2020, 9, 2005. 10.3390/jcm9062005
12. L. Giovanella, L. Bacigalupo, G. Treglia, A. Piccardo, Will 18F-Fluorocholine PET/CT Replace Other Methods of Preoperative Parathyroid Imaging? Endocrine 2021, **71**, 285–297, 10.1007/s12020-020-02487-y
13. P. Petranovi? Ov?ari?ek, L. Giovanella, I. Carrió Gasset, E. Hindié, M.W. Huellner, M. Luster, A. Piccardo, T. Weber, J.-N. Talbot, F.A. Verburg, The EANM Practice Guidelines for Parathyroid Imaging. Eur. J. Nucl. Med. Mol. Imaging. **48**, 2801–2822 (2021). 10.1007/s00259-021-05334-y
14. D. Taterra, L.M. Wong, J. Vikse, B. Sanna, P. Pękala, J. Walocha, R. Cirocchi, K. Tomaszewski, B.M. Henry, The prevalence and anatomy of parathyroid glands: a meta-analysis with implications for parathyroid surgery. Langenbecks Arch. Surg. **404**(1), 63–70 (2019). 10.1007/s00423-019-01751-8. . Epub 2019 Feb 14. PMID: 30762091; PMCID: PMC6394670
15. B. Shafiei, S. Hoseinzadeh, F. Fotouhi, H. Malek, F. Azizi, A. Jahed, F. Hadaegh, M. Salehian, H. Parsa, H. Javadi, M. Assadi, Preoperative ^{99}mTc-sestamibi scintigraphy in patients with primary hyperparathyroidism and concomitant nodular goiter: comparison of SPECT-CT, SPECT, and planar imaging. Nucl Med Commun. 2012;33(10):1070-6. 10.1097/MNM.0b013e32835710b6. PMID: 22825041
16. J. Yang, H. Wang, J. Zhang et al., Sestamibi Single-Positron Emission Computed Tomography/Diagnostic-quality Computed Tomography for the localization of abnormal parathyroid glands in patients with primary hyperparathyroidism: What clinicopathologic factors affect its accuracy? J. Endocrinol. Invest. **44**, 1649–1658 (2021). https://doi.org/10.1007/s40618-020-01471-7
17. G. Bianchetti, C.M.A. Cefalo, C. Ferreri, A. Sansone, M. Vitale, C. Serantoni, A. Abeltino, T. Mezza, P.M. Ferraro, De M. Spirito et al., Erythrocyte Membrane Fluidity: A Novel Biomarker of Residual Cardiovascular Risk in Type 2 Diabetes. European Journal of Clinical Investigation n/a, e14121. 10.1111/eci.14121
18. C. Lenschow, A. Wennmann, A. Hendricks, C.-T. Germer, M. Fassnacht, A. Buck, R.A. Werner, L. Plassmeier, N. Schlegel, Questionable Value of [99mTc]-Sestamibi Scintigraphy in Patients with pHPT and Negative Ultrasound. Langenbecks Arch. Surg. **407**, 3661–3669 (2022). 10.1007/s00423-022-02648-9

19. S. Gungor, F. Dede, B. Can, H. Keskin, M. Aras, T. Ones, T.Y. Erdil, H.T. Turoglu, The Value of Parathyroid Scintigraphy on Lesion Detection in Patients with Normocalcemic Primary Hyperparathyroidism. Revista Española de Med. Nuclear e Imagen Mol. (English Edition). **41**, 86–90 (2022). 10.1016/j.remnie.2020.12.007
20. R. Ciappuccini, J. Morera, P. Pascal, J.-P. Rame, N. Heutte, N. Aide, E. Babin, Y. Reznik, S. Bardet, Dual-Phase 99mTc Sestamibi Scintigraphy With Neck and Thorax SPECT/CT in Primary Hyperparathyroidism: A Single-Institution Experience. Clin. Nucl. Med. **37**, 223–228 (2012). 10.1097/RLU.0b013e31823362e5
21. N. Khorasani, A. Mohammadi, Effective factors on the sensitivity of preoperative sestamibi scanning for primary hyperparathyroidism. Int. J. Clin. Exp. Med. **7**(9), 2639–2644 (2014). PMID: 25356120; PMCID: PMC4211770

Figures

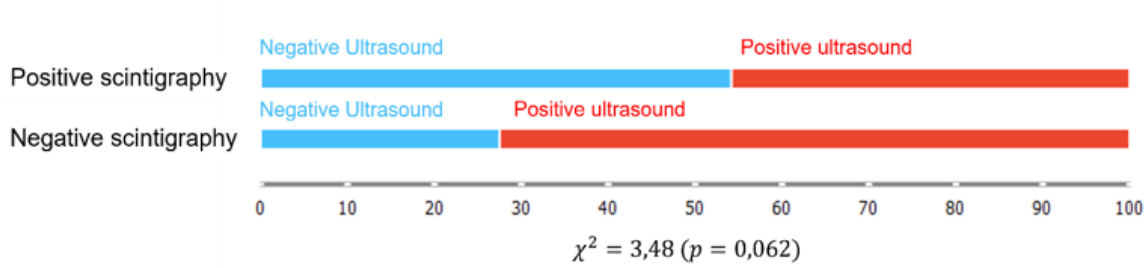


Figure 1

Relationship between neck ultrasound result and scintigraphy outcome. The graph shows the fraction of patients with positive (in red) or with negative (in blue) NUS, respectively, belonging to the positive or negative scintigraphy group.

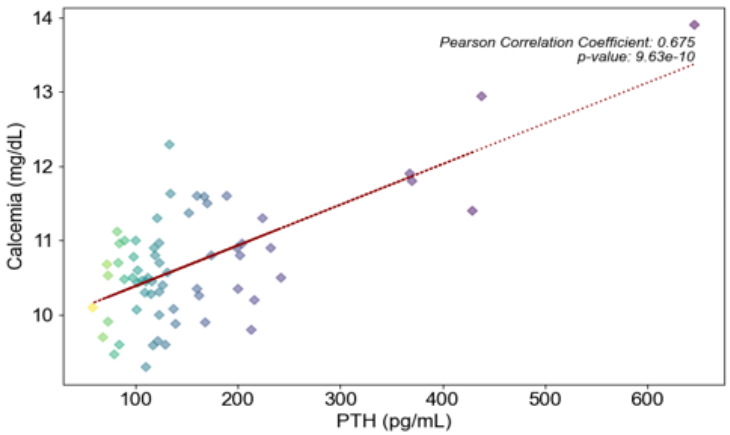


Figure 2

Relationship between calcemia and parathyroid hormone (PTH) levels. Calcemia (y-axis, in mg/dL) is represented as as function on PTH values (x-axis, in pg/mL). Each data point on the graph corresponds to an individual patient within our study cohort. The dotted line on the graph represents the linear regression line fitted to the data points. The PCC is reported along the graph, together with the corresponding p-value.

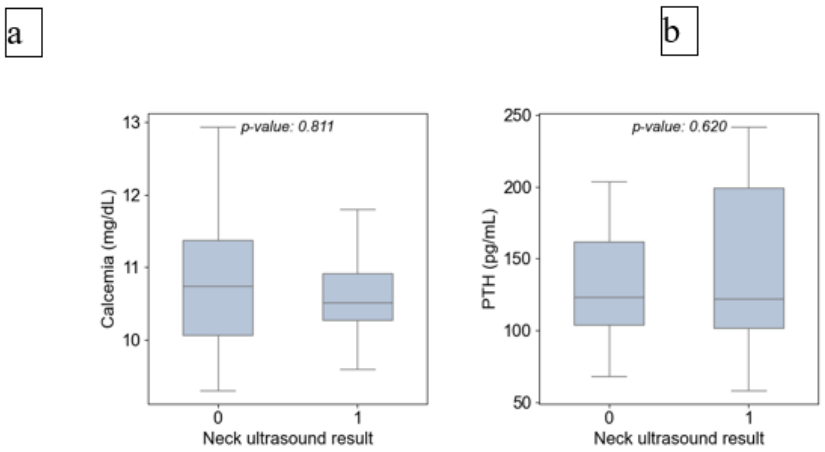
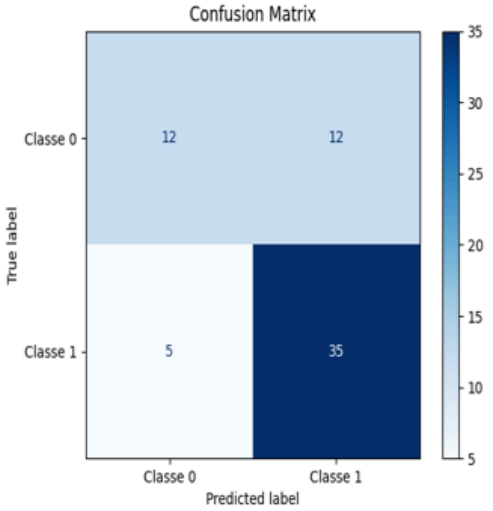
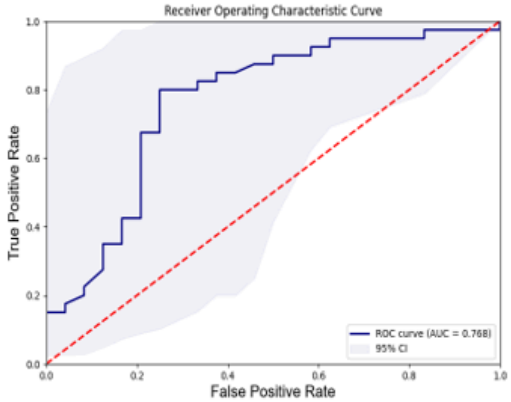


Figure 3

Representative levels of calcemia and parathyroid hormone (PTH) as a function of NUS result. Levels of calcemia (**a**) and PTH (**b**) are shown in the box plot for patients with negative (0) and positive neck ultrasound (1), respectively. Calcemia and PTH are reported on the y-axis, in mg/dL and pg/mL. p-values obtained from Student's t-test are indicated along with the box plots. p-value < 0.05 is considered statistically significant.



(a)



(b)

Figure 4

Metrics for model evaluation. The confusion matrix in (**a**) provides a detailed representation of true positive, true negative, false positive, and false negative predictions. The ROC curve represented in (**b**) shows the accuracy of the selected logistic regression model (Model 2) in identifying individuals with higher probability of a false negative scintigraphy result. The 95% confidence interval is colored in light blue, and the value of AUC is reported in the legend.